

=====

**SORPTION
AND ION-EXCHANGE PROCESSES**

=====

New Carbon Aerogels Fabricated from Polymeric Materials and Their Properties

S. S. Stavitskaya, V. E. Goba, A. N. Tomashevskaya, and N. N. Tsyba

Institute of Sorption and Endoecology Problems, National Academy of Sciences of the Ukraine, Kiev, Ukraine

Received June 16, 2004; in final form, April 2005

Abstract—Electron microscopy and adsorption-structural, X-ray phase, and thermal analyses were used to determine the density, porosity, microstructure, electrical conductivity, and reactivity of new carbon aerogels based on phenol-formaldehyde polymers.

Low-density carbon materials, carbon aerogels (CA), were first produced by pyrolysis of organic aerogels [1–3]. All the subsequent studies were devoted to synthesis and analysis of the structural parameters and adsorption and electrical properties of carbon aerogels [4–8]. Carbon aerogels were obtained by the classical scheme in three steps: sol-gel polymerization of organic oligomers (synthesis of organic aerogels), high-efficiency drying in a flow of CO₂, and high-temperature carbonization of the resulting organic aerogels (synthesis of carbon aerogels).

In the first stage, the influence exerted by the relative content of starting components [4], thermal stability of chosen resins [5] and solvents (mostly alcohols) [6], and presence in the course of polymerization of catalysts [Ca(OH)₂, Na₂CO₃] [7] and cross-linking agents (e.g., melamine) [8] on the final properties of the carbon aerogels obtained was studied in detail. Commonly, resorcinol-formaldehyde, phenol-furfural, melamine-formaldehyde, polyurethane, and, less frequently polyvinyl chloride systems are used as starting components [9].

The interest in materials of the aerogel type is due to the wide opportunities for their use in chemical technology and electrical engineering, provided by their uniquely high porosity, electrical conductivity, corrosion and acid resistance, and biological stability [3, 4, 7, 8, 10–14].

Published studies have been mainly concerned with methods for synthesis of carbon aerogels and properties of these materials, with little attention given to the possibility of controlled variation of the porous structure and chemical nature of the surface of the re-

sulting carbon aerogels, e.g., by special treatment and directional modification. Therefore, a search for new ways of synthesis and new forms of carbon aerogels is a matter of current interest.

EXPERIMENTAL

This study is concerned with properties of new carbon aerogels prepared from phenol-formaldehyde oligomers (PFO) and with changes in the structural parameters, porosity, nature of the surface, and electrical properties upon their thermal treatment (activation) in the atmosphere of CO₂ and oxidation with nitric acid.

Carbonized products differing in degree of branching, porosity, and other structural parameters and texture can be obtained by using in synthesis the phenol-formaldehyde resin, which can form 3D hexagonal carbon networks in carbonization, and various relative amounts of the same components and additives.

PFO was carbonized in a flow of N₂, with the treatment time of the starting polymer varied within 2–4 h and the carbonization temperature gradually elevated from 400 to 600°C. The activation was done in the atmosphere of CO₂ at 850°C during a varied time and the oxidation was performed with concentrated HNO₃ [15]. The porous structure was characterized by electron microscopy and adsorption-structural analysis by sorption of benzene vapor and H₂O, and low-temperature (77 K) sorption of N₂. The gas-chromatographic method of thermal desorption of argon was used to measure the specific surface area S_{sp} of the samples studied. The nature and amount of oxygen-containing functional surface groups was determined by chemical

Table 1. Sorption parameters of carbon aerogels prepared from phenol-formaldehyde oligomers and selected activated carbons*

Sample	d , mg cm ⁻³	W_s	U_Σ	Sample	d , mg cm ⁻³	W_s	U_Σ
CA-1	20	0.20	1.1	CA ₂ -A	115	0.33	8.4
CA-2	90	0.17	2.6	Raw PF	920	0.12	1.4
CA-3	145	0.20	3.4	PF-A	690	0.50	1.8
CA ₁ -A	125	0.34	41.9	BAC	250	0.34	1.8

* CA₁-A and CA₂-A, aerogels activated in a flow of CO₂ for 2 and 4 h, respectively; PF-A, carbon activated from phenol-formaldehyde resin; BAC, birch activated carbon.

Table 2. Physicochemical parameters of the initial (raw PF) and activated phenol-formaldehyde (PF-A) carbons and carbon aerogels synthesized on their basis*

Sample	d , mg cm ⁻³	W_s	V_{micro}	V_{meso}	V_{macro}	S_{sp} , m ² g ⁻¹	E_o , kJ mol ⁻¹	$B \times 10^6$	W_o , cm ³ g ⁻¹
Raw PF	920	0.12	0.02	0.01	–	150	–	–	–
PF-A	690	0.34	0.09	0.14	–	170	–	–	–
CA-1	30	0.17	0.100	0.036	0.875	228	16.6	1.18	0.15
CA-2	45	0.20	0.178	0.047	–	235	17.0	1.50	0.19
CA-3	60	0.22	0.176	0.079	0.662	265	23.6	0.66	0.14
CA-4	70	0.25	0.246	0.064	–	300	24.2	0.66	0.14
CA-5	85	0.22	0.178	0.093	0.660	370	31.2	0.82	0.22
CA-6	140	0.20	0.141	0.035	0.590	418	23.6	0.66	0.11
CA ₁ -A	140	0.34	0.204	0.006	0.550	358	27.4	1.30	0.09
CA ₂ -A	150	0.35	0.186	0.032	0.590	407	10.6	1.80	0.10
CA-O	73	0.33	0.196	0.064	0.599	300	–	–	–

* CA-1–CA-6, carbon aerogels, carbonizates of phenol-formaldehyde resins of different compositions and densities; CA₁-A and CA₂-A, carbon aerogels additionally activated in a flow of CO₂ for 2 and 4 h, respectively; CA-O carbon aerogel oxidized in the liquid phase with nitric acid.

titration [15]. The structure and reactivity of carbon aerogels was also subjected to X-ray phase and thermographic analyses [16, 17].

Phenol-formaldehyde resins with prescribed texture and varied ratio of the components were used as starting materials to obtain, after carbonization in the atmosphere of N₂, carbon aerogels with a widely variable apparent density d , which was in the range 20–150 mg cm⁻³ for different samples. It should be noted that the density of the carbon aerogel samples obtained is considerably lower than that of an untreated, additionally expanded graphite ($d = 350$ mg cm⁻³) and aerosils (150–180 mg cm⁻³).

Compared with the conventional activated carbons, synthetic low-density carbon aerogels exhibit rather high sorption parameters (Table 1) (specific volume of sorption pores, W_s , found by the desiccator method from the of sorption of a benzene vapor is 0.35 cm³ g⁻¹)

and a high total porosity U_Σ [16], which, in some cases, exceeds that of BAC and activated phenol-formaldehyde carbons by an order of magnitude (Table 1) [15, 18].

Electron-microscopic studies demonstrated that carbon aerogels have a strongly inhomogeneous microcellular structure. The surface of the aerogels is pierced by coarse macropores (2×10^3 – 1×10^4 nm and more, up to several tens of micrometers, depending on the sample density). It is the presence of a large number of macropores that is responsible for the high total porosity and 90–95 : 100 ratio of the apparent and true densities. The electron-microscopic data obtained were used to calculate the wall thickness of carbon aerogels, which varied widely, from 10 to 600 nm.

As indicated by the sorption data (for benzene and water vapor, Table 2), carbonizates of carbon aerogels

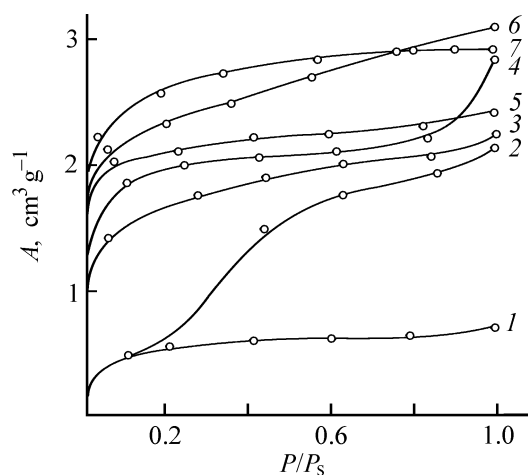


Fig. 1. Isotherms of benzene vapor sorption by carbon aerogels with different densities and varied chemical nature of the surface and by activated carbon prepared from a phenol-formaldehyde resin, obtained on an adsorption-gravimetric setup (McBain balance). (*A*) Adsorption and (P/P_s) relative pressure. CA sample, density (mg cm^{-3}): (1) oxidized CA-O, 30; (2) CA, 30; (3) CA, 45; (4) CA, 85; (5) CA, 140; (6) CA₁-A (activated) 140; and (7) activated carbon prepared from a phenol-formaldehyde resin.

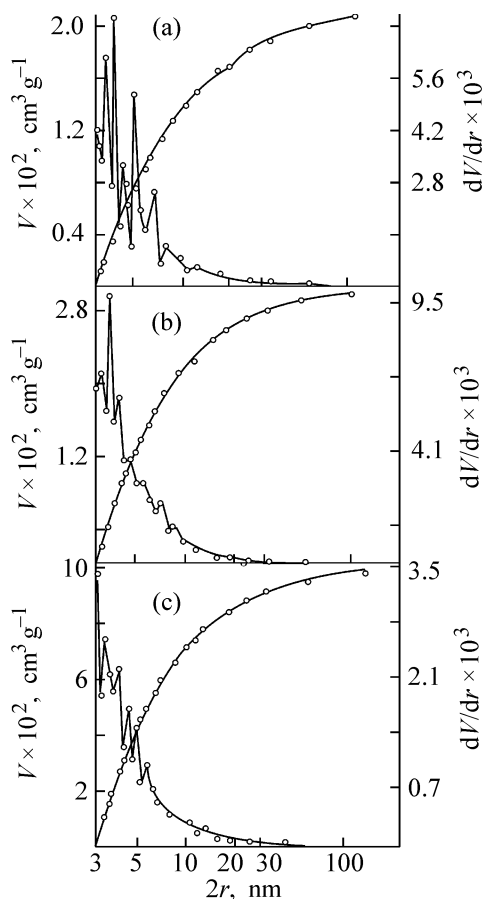


Fig. 2. Differential (dV/dr) and integral (V) distributions of pores over radii r in (a) initial aerogel, (b) activated CA, and (c) oxidized CA-O.

of the same nature have, in contrast to low-porosity raw carbon based on phenol-formaldehyde resins, a rather developed system of micropores, which is formed already in the carbonization stage. In activated carbons prepared from phenol-formaldehyde resins, micropores appear only in the course of activation.

The benzene sorption isotherms obtained (Fig. 1) and the structural parameters calculated from these isotherms (Table 2) indicate that all the carbon aerogel samples contain micro- (V_{micro}), meso- (V_{meso}), and macropores (V_{macro}), whose volume V strongly depends on the sample density. An increase in the density of carbon aerogels makes larger the volume of the sorption space (amount A of adsorbed benzene vapor, Fig. 1), that of mesopores (V_{meso}), and specific surface area S_{sp} .

An additional activation of carbon aerogels also makes higher their sorption capacity via development of micropores, with, however, strongly decreasing mesoporosity.

The presence of micropores in carbon aerogels is confirmed by the values of the main parameters of the microporous structure [19], structural constants B and W_0 in the equation of the theory of volume filling of micropores and the characteristic adsorption energy E_0 , which are found from data on water sorption at $P/P_s = 1$ (Table 2). Constant W_0 is the limiting volume of the adsorption space, and constant B characterizes the size of micropores [19]. An increase in constant B indicates that micropores become larger; at small B , W_0 is close to the volume of micropores.

As the density of carbon aerogels increases, the surface area of the samples becomes larger. In some cases, it reaches values typical of activated carbons. An increase in the characteristic energy E_0 , with a simultaneous decrease in the structural constant B , indicates that small micropores and even ultramicropores are predominant in the structure of aerogels with a sufficiently high density ($d \approx 100 \text{ mg cm}^{-3}$) [15, 18].

The presence of a microporous structure in the carbon aerogels synthesized is also confirmed by the results of a study of their structural-sorption parameters for N_2 , obtained on a Quantachrome NOVA 2200E high-speed gas sorption analyzer. Figures 2a–2c show pore radius distributions for, respectively, the starting sample (carbonizate), activated CA–A, and oxidized CA–O, which were calculated using the Barrett–Joyner–Halenda (BJH) method [20]. The initial nonacti-

Table 3. Structural-sorption parameters of some of the samples studied, found from the low-temperature adsorption of nitrogen (BJH method)*

Sample	A , $\text{cm}^3 \text{g}^{-1}$, at $P/P_s = 1$	Average pore width, nm	V_{micro} , $\text{cm}^3 \text{g}^{-1}$	S		E , kJ mol^{-1}
				S_{micro}	S	
				$\text{m}^2 \text{g}^{-1}$		
Raw PF	12.0	8.2	0.0	6.5	6.2	3.2
CA-A	21.0	6.6	0.2	8.9	630	3.9
CA-O	280.0	2.4	0.4	10.1	969	11.0

* A , nitrogen adsorption at 77 K; V_{micro} , volume of micropores, calculated by the BJH method; S_{micro} , surface area of micropores; S , total surface area; and E , adsorption energy.

vated aerogel contains micropores of various sizes, whereas in the activated and oxidized sample, only 3–5-nm micropores were observed, i.e., the carbon aerogels synthesized are nanosize and uniformly microporous, which is a rather valuable property as regards their practical application. Table 3 lists the structural-sorption parameters of some of the samples under study, found from the low-temperature adsorption of N_2 , using the BJH method.

In order to study the possibility of controlling the structure and chemical nature of the surface of carbon aerogels and imparting new properties to these materials, the reactivity and thermal stability of carbon aerogels were examined in various oxidizing media (CO_2 , O_2) at different temperatures.

To develop the microporosity and raise the sorption capacity, samples of varied density were subjected to a high-temperature (850°C) activation with carbon dioxide. In doing so, the main activation parameters were determined and data on how the density of carbon aerogels varies in the process (Fig. 3) were obtained.

High-temperature treatment of finished samples of carbon aerogels in the atmosphere of CO_2 makes higher the total porosity, number of micropores, absorption capacity for benzene and water, and S_{sp} , but diminishes the number of meso- and macropores (Table 2). As the BJH method yields clear-cut data on the content of micro- and mesopores [20], the volume of macropores in the carbon materials studied was determined [20] as the difference between the total volume of pores, found from the moisture absorption capacity of the carbons, and the maximum volume of sorbed benzene, W_s . The following specific features of the process of thermal treatment of the carbon aerogels prepared are noteworthy. It was found, in particular, that d is virtually the same for samples

with a low initial density, subjected to activation for different periods of time (Fig. 3). At the same time, the density of samples with an initial density $d > 50 \text{ mg cm}^{-3}$ decreases during thermal treatment till a certain instant of time, presumably via burning-out of the most reactive amorphous part of carbon and further development of porosity, whereas at longer treatment, a structural transformation of the skeleton occurs and the density increases to nearly its initial value. This may be due to changes in the texture of carbon aerogels in prolonged thermal treatment.

Thus, the optimal activation conditions and, in particular, the time of activation for aerogels of varied density, at which the quality of the aerogels is markedly improved, were revealed.

The reactivity of carbon aerogels toward oxygen was determined from the results of a thermogravimet-

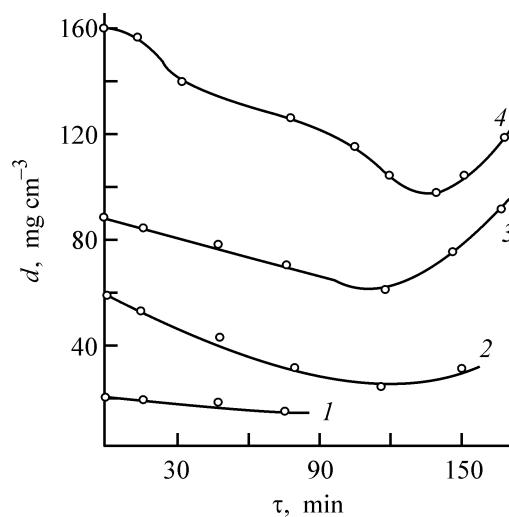


Fig. 3. Kinetics of variation of the apparent density d of carbon aerogels. (τ) Activation time. Carbon aerogel: (1) CA-1, (2) CA-3, (3) CA-5, and (4) CA₂-A.

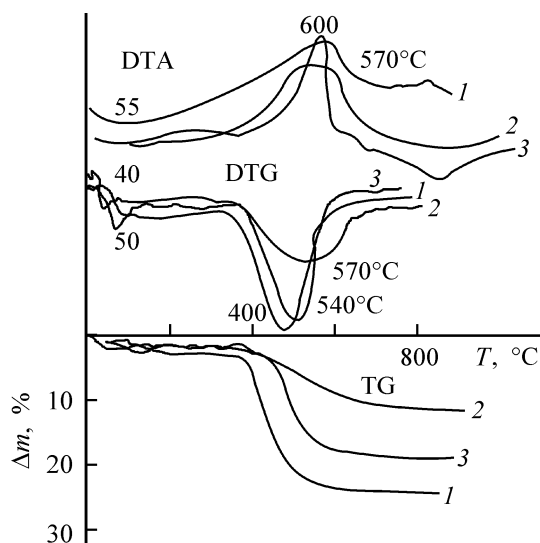


Fig. 4. Thermograms of carbon aerogels, obtained in air. (T) Temperature and (Δm) loss of mass. Sample, d (mg cm^{-3}): (1) starting carbonizates of CA-1, 30; (2) CA-6, 140; and (3) activated CA₂-A, 140.

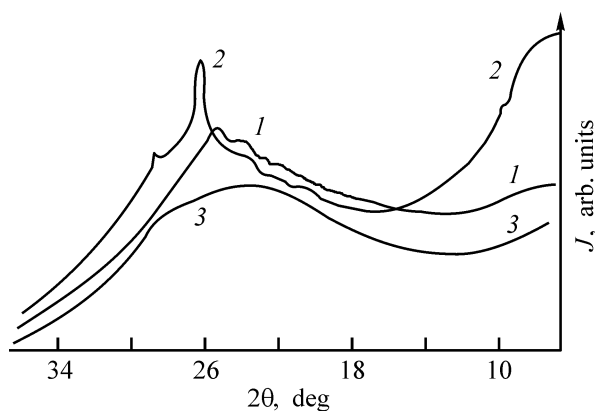


Fig. 5. X-ray diffraction patterns of carbon aerogels and raw phenol-formaldehyde carbon. (J) Signal intensity and (2θ) Bragg angle; the same for Fig. 6. CA sample, d (mg cm^{-3}): (1) CA-3, 60; (2) CA-6, 140; and (3) raw PF.

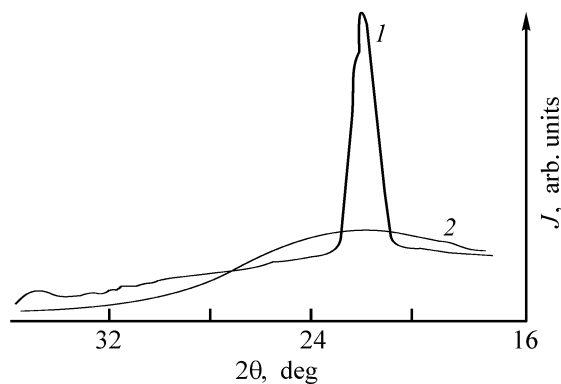


Fig. 6. X-ray diffraction patterns of (1) activated aerogel CA₁-A and (2) activated phenol-formaldehyde carbon PF-A.

ric analysis (Fig. 4), performed both in air and in an inert atmosphere (Ar) [21] on an MOM derivatograph (Hungary). The weighed portions were 100 mg, the temperature was raised at a rate of 5 deg min^{-1} . Heating of carbon aerogels first leads to a minor endothermic effect at $40\text{--}55^\circ\text{C}$. This effect should be attributed to removal of sorbed water. As the temperature is raised to $540\text{--}600^\circ\text{C}$, the carbon mass of all of the samples studied burns out, which is accompanied by an exothermic effect. The rates of carbon destruction at different times of contact with the oxidant are not the same, which is indicated by the TG curves showing the loss of the carbon mass. The higher the density of carbon aerogel samples, the better their thermal stability: a low-density sample (curve 1) burns out faster than do aerogels with $d = 140 \text{ mg cm}^{-3}$ (curves 2, 3). In the inert medium, the thermal stability of carbon aerogels is considerably higher.

The reactivity of carbon materials depends not only on their porous structure, but also on the forms in which carbon exists in their structure and on its valence state.

According to the results of an X-ray phase analysis on a DRON-2 instrument, the carbon skeleton of low-density aerogels ($d = 30\text{--}50 \text{ mg cm}^{-3}$) is mostly composed of disordered amorphous carbon.

In this case, however, the intensity of the diffuse halo increases with the sample density and diffraction peaks appear on its background, which points to a crystalline ordering of carbon, compared with the very diffuse halo from activated carbon of the same nature (Fig. 5). In the X-ray scattering curves of carbonizates of aerogels with a comparatively high density ($d > 100 \text{ mg cm}^{-3}$), the intensity of the diffraction peaks grows, which points to predominance of the crystalline form size and larger of carbon crystallites.

Particularly strongly different are the X-ray spectra of activated samples of carbon aerogels and phenol-formaldehyde carbon (Fig. 6). The X-ray diffraction patterns of an activated aerogel show a clearly pronounced diffraction peak of the 002 band, which indicates a considerable increase in the content of crystalline carbon in the microstructure upon activation, untypical of the ordinary activated carbon.

The position of the 002 band in the X-ray diffraction patterns of aerogel samples and its halfwidth were used to calculate by the Warren equation [22] the average size of carbon crystallites in the micro-

structure of the aerogels: L_a , height of packets of atomic networks; L_d , diameter of these packets (Table 4).

As can be seen in Table 4, the parameters of the microstructure of carbon aerogels significantly differ from the same parameters of the known carbon materials (e.g., in the larger interplanar spacing $L = 4.1 \text{ \AA}$). This fact can account for the discrepancy between the true densities of activated phenol-formaldehyde carbon (1.65 g cm^{-3}) and of the carbon skeleton of carbon aerogels ($0.9\text{--}1.25 \text{ g cm}^{-3}$).

Growth of crystallites and their ordering are favored by an additional high-temperature activation, which is indicated by an increase in the height of atomic-network packets to 60 \AA and in their diameter to 115 \AA at a constant interplanar spacing.

The considerable fraction of crystalline carbon in the carbon aerogels synthesized leads to their higher (compared with the corresponding samples of PF-A activated carbon) electrical conductivity (Table 5).

As is known [15], the conduction in carbons as graphite bodies is mainly effected by π -electrons moving along planes of hexagonal networks (via the system of conjugated bonds). The electrical resistance of powdered carbon materials is determined, as in other crystalline bodies, by their internal microstructure and contacts (barriers) between particles. The electrical resistance of the barriers depends both on the state of the particle surface (presence of functional groups, adsorbed substances, impurities on the surface) and on the particle size and pressure applied to the powder [21, 23]. To exclude the influence of the last factors, which are not related to the nature of a material under study, the electrical resistance was measured under identical conditions (grain size, pressure, etc.).

To determine the electrical resistance, carbon aerogels and carbons were taken in the form of a ground ($D = 0.25 \text{ mm}$) freely poured powder. A weighed portion of a powder was placed in a 1-cm-long porcelain tube with an inner diameter of 6 mm and the tube was clamped between two metallic cylinders. The measurements were carried out under constant pressure at 20°C in the ac mode. The electrical resistance was determined by the voltmeter-ammeter method [23]. A G3-43 generator working in the frequency range $0.15\text{--}30 \text{ MHz}$ served as a voltage source. The voltage drop across a sample was measured with a V3-4 valve voltmeter.

As demonstrated by the data obtained, the highest electrical conductivity χ (lowest electrical resistivity ρ) was observed for low-density carbon aerogels. As the density of the aerogels becomes higher, their elec-

Table 4. Comparative characteristics of microstructures of various carbon materials

Carbon material	L	L_c	L_a
	\AA		
Graphite	3.34–3.35	200	6.69
Carbon blacks, fossil coals, sugar coke	3.44	26–28	9–12
PF-A	3.5–3.6	58–83	22–24
CA	4–4.1	22–46	11–21
CA ₁ -A	–	15	28
CA ₂ -A	–	115	57

Table 5. Electrical properties of carbon materials

Sample	$d, \text{ mg cm}^{-3}$	$\rho, \Omega \text{ cm}$	$\chi, \Omega^{-1} \text{ cm}^{-1}$
Aerogel	30	20.5	4.9×10^{-2}
	45	22.1	4.4×10^{-2}
	70	41.7	2.4×10^{-2}
	85	58.7	1.7×10^{-2}
	120	99.5	1.1×10^{-2}
CA ₁ -A	140	32.5	3.1×10^{-2}
CA ₁ -A (H ₂)*	140	68.2	1.4×10^{-2}
Raw PF	–	247	4.1×10^{-3}
PF-A**	–	132	7.6×10^{-3}

* Activated CA additionally treated in a flow of H₂ at 850°C to remove possible surface oxides.

** Activated in a flow of CO₂.

trical resistance increases, possibly because of the higher content ratio of amorphous and crystalline carbon in the microstructure of the aerogels. In this case, however, ρ of carbon aerogels is an order of magnitude lower than that of activated carbon. Additional activation of carbon aerogels (Table 5, samples CA₁-A and CA₂-A) diminishes their electrical resistance.

It should be noted that the possibility of obtaining carbon aerogels with a sufficiently high electrical conductivity is rather important for technology, especially for fabrication of molded articles of prescribed configuration on the basis of carbon aerogels.

It is known [15] that presence of acidic surface functional groups on the carbon surface strongly changes not only the sorption and catalytic properties of carbon materials, but also the electrical parameters and performance of articles containing various modifications of free carbon.

In this context, the possibility of changing the chemical nature of the surface of carbon aerogels and

obtaining their oxidized forms by treatment of activated carbon aerogels with concentrated HNO₃ solutions was also analyzed [15]. In the process, samples with a high cation-exchange capacity of up to 4 mmol g⁻¹ and different compositions of surface functional groups with varied acidity were prepared. It should be noted that preparation of oxidized carbons with SEC exceeding 2 mmol g⁻¹ is commonly accompanied by destruction of the carbon substance to give fulvic acids and coloring humic acids [15], which is untypical of oxidized aerogels.

The relative contents of surface functional groups in carbon aerogels, obtained here, approximately correspond to the known distributions of such groups, observed on ordinary oxidized carbons [15]. The change of the chemical nature of the surface in oxidized carbon aerogels, compared with activated carbons of the same density, is also confirmed by the results of a thermogravimetric analysis. These data indicate that the onset of the reaction between oxygen and the carbon mass is observed in oxidized carbon aerogels at a higher temperature (540–560°C) than that in activated carbons (440–470°C). Presumably, this results from the shielding effect of oxygen-containing surface functional groups. It should be noted that there is no evidence concerning the synthesis and analysis of properties of their oxidized forms in the literature devoted to carbon aerogels.

CONCLUSIONS

(1) New low-density carbon materials, aerogels with a widely controllable apparent density (20–150 mg cm⁻³), were synthesized from phenol-formaldehyde polymers by carbonization.

(2) It was shown that the carbon aerogels synthesized show high sorption capacity (for benzene, water, and nitrogen) and total porosity. In addition to a large number of macropores, the materials under study possess a rather well-developed microporous structure. In contrast to that of ordinary carbons based on phenol-formaldehyde oligomers, this microporous structure is formed already in the carbonization stage and leads to a high sorption capacity and large specific surface area comparing well with that in industrial carbons.

(3) An X-ray phase analysis demonstrated an increased content of crystalline carbon in the microstructure of carbon aerogels after their activation, which is untypical of the ordinary activated carbon. The samples synthesized also differ from those of ordinary activated carbon in the parameters of microstructure,

considerably larger interplanar spacings (up to 4.1 Å), which leads to their lower true density, compared with that of ordinary carbons based on the phenol-formaldehyde resin.

(4) It was found that the aerogel samples studied exhibit a high electrical conductivity typical of carbon materials of this kind. The electrical conductivity exceeds that of phenol-formaldehyde carbons by a factor of 2–5.

(5) Cation-exchange (oxidized) forms of carbon aerogels with a high sorption capacity (SEC of up to 4 mm g⁻¹) and various compositions of acidic surface functional groups were obtained. It was established that, when such an exchange capacity is reached, no destruction of the carbon substance occurs and no coloring humic and fulvic acids are formed. This points to a high chemical stability of the carbon skeleton obtained.

(6) The study of the properties of the carbon aerogels synthesized made it possible to suggest that materials of this kind can find use as effective adsorbents, various filter media, fillers of chromatographic columns, etc.

REFERENCES

1. Pekala, R.W., *J. Mater. Sci.*, 1989, vol. 24, no. 9, pp. 3221–3231.
2. US Patent 476778.
3. Pekala, R.W., Farmer, J.C., Alviso, C.T., and Tran, T.D., *J. Non-Cryst. Solids*, 1998, vol. 225, no. 1, pp. 74–80.
4. Petricevic, M., Glora, M., and Fricke, J., *Carbon*, 2001, vol. 39, no. 6, pp. 857–867.
5. Yamashita, J., Ojima, T., Hatori, H., and Yamada, Y., *Carbon*, 2003, vol. 41, no. 2, pp. 285–295.
6. Guotong Qin and Shucaï Guo, *Carbon*, 2001, vol. 39, no. 12, pp. 1935–1937.
7. Thery, A., Clinard, C., Beguin, F., *et al.*, *Proc. Int. Conf. on Carbon, 2002, Beijing, China*, CD-ROM SBN 7-900362-03-7/G03.
8. Rui Zang, Zhihong Li, Yiao Xu, *et al.*, *Proc. Int. Conf. on Carbon, September 15–20, 2002, Beijing, China*, CD-ROM SBN 7-900362-03-7/G03.
9. Thorikawa, T., Ogawa, K., Mizuno, K., *et al.*, *Carbon*, 2003, vol. 41, no. 3, pp. 465–472.
10. Petricevic, R., Reichenauer, G., and Fricke, J., *J. Non-Cryst. Solids*, 1998, vol. 225, no. 1, pp. 41–51.
11. Gilow, K.M. and Shapovalova, L.N., *Polym. Degrad. Stab.*, 1992, vol. 38, no. 1, pp. 27–34.
12. Mitrofanov, V.D., Manakov, A.I., and Shveikin, G.P., *Karbidy i materialy na ikh osnove* (Carbides and

- Materials on Their Basis), Kiev: Inst. Probl. Materialoved., Akad. Nauk SSSR, 1991.
13. Noriko Yoshizawa, Yasushi Soneda, Hiroaki Hatori, and Yohko Hanzawa, *Proc. Int. Conf. on Carbon, July 6–10, 2003, Oviedo, Spain*, CD-ROM JSBN 0-9 674 971-249 674 972.
 14. Li, W.C., Lu, A.H., and Guo, S.C., *Carbon*, 2001, vol. 39, no. 12, pp. 1989–1994.
 15. Tarkovskaya, I.A., *Okislennyi ugol'* (Oxidized Carbon), Kiev: Naukova Dumka, 1981.
 16. Nefedov, V.I., *Rentgenoelektronnaya spektroskopiya khimicheskikh soedinenii* (X-ray Photoelectron Spectroscopy of Chemical Compounds), Moscow: Khimiya, 1984.
 17. Larina, A.A., Tarkovskaya, I.A., Zakolodyazhnaya, O.V., *et al.*, *Teor. Eksperim. Khim.*, 1984, no. 4, pp. 496–501.
 18. Dubinin, M.M., *Poristaya struktura i adsorbtsionnye svoistva aktivnykh uglei* (Porous Structure and Adsorption Properties of Activated Carbons), Moscow: Voen. Akad. Khim. Zashchity, 1965.
 19. Kolyshkin, D.A. and Mikhailova, K.K., *Aktivnye ugli: Spravochnik* (Activated Carbons: Reference Book), Leningrad: Khimiya, 1993.
 20. Gregg, S.J. and Sing, K.S., *Adsorption, Surface Area and Porosity*, London: Acad., 1982.
 21. Stavitskaya, S.S., Larina, A.A., Tarkovskaya, I.A., and Zakolodyazhnaya, O.V., *Khim. Tverd. Tela*, 1990, no. 5, pp. 111–113.
 22. Spiridonov, E.P., Barykin, B.M., Drozdov, R.Ya., *et al.*, *Strukturnaya khimiya ugleroda i uglei* (Structural Chemistry of Carbon and Coals), Kasatochkin, V.I., ED., Moscow: Nauka, 1969.
 23. Tarkovskaya, I.A., Kozub, G.M., Goba, V.E., and Stavitskaya, S.S., *Ukr. Khim. Zh.*, 1978, vol. 44, no. 5, pp. 489–493.